ASED http://e-ASED.org
Animal Systematics, Evolution and Diversity

Anim. Syst. Evol. Divers. Vol. 34, No. 3: 143-151, July 2018
https://doi.org/10.5635/ASED.2018.34.3.143

First Record of *Amphisiella milnei* (Ciliophora, Stichotrichida) from Korea

Jung Min Choi[1], Jae-Ho Jung[2], Young-Ok Kim[1,*]

[1]Korea Institute of Ocean Science & Technology (KIOST), Busan 49111, Korea
[2]Department of Biology, Gangneung-Wonju National University, Gangneung 25457, Korea

ABSTRACT

A marine ciliate *Amphisiella milnei* (Kahl, 1932) Horváth, 1950 was discovered from the tidal pool of Baekdo Island, South Korea. The existence of extra cirri between leftmost frontal cirrus and buccal cirrus discriminates this species from its congeners. Its morphological features are described as follows: body size *in vivo* 110−130×35−45 μm; elongate rectangular to elliptical in shape; two large and several small ring-shaped structures; yellowish cortical granules arranged irregularly on ventral side but longitudinally along dorsal kineties on dorsal side; 34−40 adoral membranelles, 3 frontal cirri, 1 buccal cirrus, 1 parabuccal cirrus, usually 2 extra cirri behind leftmost frontal cirrus, and 3 frontoventral cirri; amphisiellid median cirral row composed of 25−31 cirri with 27−36 left and 27−44 right marginal cirri; usually 5 transverse cirri and 2 pretransverse cirri with 7 dorsal kineties; two macronuclear nodules. In addition to, 18S rDNA sequence of *A. milnei* was analyzed to understand its phylogenetic relationship.

Keywords: 18S rDNA, *Amphisiella*, marine hypotrich, phylogeny, South Korea, taxonomy

INTRODUCTION

The main diagnostic characteristics of the genus *Amphisiella* are an amphisiellid median cirral row (ACR) and the number of dorsal kinety (i.e., >3). Its ACR actually consists of two cirral rows, anlagen V and VI. During morphogenesis, these two rows then migrate to form a single-combined row (Berger, 2008).

In the past, more than 30 species/subspecies have been assigned to this genus, however currently only eight species (i.e., *A. annulata*, *A. candida*, *A. capitata*, *A. milnei*, *A. ovalis*, *A. pulchra*, *A. sinica*, and *A. turanica*) showing homogeneous pattern have remained in *Amphisiella* (Li et al., 2007; Berger, 2008; Chen et al., 2013; Li et al., 2016). This genus was considered as monophyly (Li et al., 2007; Berger, 2008) before the recent reports of four species including two new species *A. candida* and *A. pulchra* by Chen et al. (2013) and redescribed *A. milnei* and new species *A. sinica* by Li et al. (2016). Polyphyly of *Amphisiella* group was first suggested by Chen et al. (2013). Their molecular analyses showed low supporting values on the genus *Amphisiella* because of the basal placement of *A. candida*, which finally split away from the others later (see below). The secondary structure of helix E10-1 in V2 region is also different between *A. candida* and other *Amphisiella* species. Subsequently, Huang et al. (2016) and Li et al. (2016) divided *Amphisiella* into two groups (i.e., *A. annulata*−*A. pulchra*−*A. sinica* vs. *A. milnei*−*A. candida*) based on morphology and molecular analyses. However, the DNA sequence of the type species *A. capitata* is not available yet to establish a new genus for between the two groups.

Here, we collected a population of *Amphisiella milnei* from an deserted island known as "Baekdo Island", South Korea. Morphological and molecular analyses were performed for this Korean population. Its morphological and molecular features described here.

MATERIALS AND METHODS

Sample collection and enrichment

Amphisiella milnei was collected from tidal pool of Baekdo Island (34°03′13.80″N 127°35′00.60″E), South Korea in Jun 2012. The species was cultured in ambient sea water. Rice grains were added to proliferate bacteria as food resource

*To whom correspondence should be addressed
Tel: 82-51-664-3331, Fax: 82-51-955-3981
E-mail: yokim@kiost.ac.kr

eISSN 2234-8190

for the ciliate. Raw cultures were maintained in Petri dish and incubated at room temperature.

Morphological observation and identification

Specimens were observed under a Zeiss Stemi DV4 (Zeiss, Göttingen, Germany) and a light microscope (Zeiss Imager. A2; Zeiss) at magnifications ranging from 100× to 1,000×. Protargol impregnation was performed to observe the infraciliature as described previously (Wilbert, 1975; Foissner, 1991). Terminology and classification are according to Berger (2008) and Lynn (2008).

PCR amplification and sequencing

Living cells were washed several times with filtered sea water. Each individual was isolated into microcentrifuge tube for DNA extraction. Genomic DNA was extracted using a RED-Extract-N-Amp Tissue PCR Kit (Sigma, St. Louis, MO, USA). A modified EukA (5′-CTG GTT GAT YCT GCC AGT-3′) forward primer (Jung et al., 2012) and LSU rev4 (5′-GTT AGA CTY CTT GGT CCG TG-3′) reverse primer (Sonnenberg et al., 2007) were used for PCR amplification of 18S rDNA. Optimized PCR conditions were as follows: denaturation at 94°C for 3 min, 35 cycles of denaturation at 94°C for 30 s, annealing at 58°C for 30 s, extension at 72°C for 3 min, and a final extension step at 72°C for 7 min. The following two internal primers were used for sequencing: 18S+790v2 (5′-AAA TTA KAG TGT TYM ARG CAG-3′) and 18S-300 (5′-CAT GGT AGT CCA ATA CAC TAC-3′) (Jung and Min, 2009). DNA sequencing was performed using an ABI 3700 sequencer (Applied Biosystems, Foster City, CA, USA). These sequences are deposited in GenBank under the accession numbers MH645737, MH645741, and MH645742.

Molecular analyses

The sequence fragments of 18S rDNA newly obtained from each sequencing primer were assembled using Geneious v7.1.5 (Drummond et al., 2014). The consensus sequence was aligned with related sequences retrieved from GenBank using T-Coffee v10.00 r1613 (Notredame et al., 2000). Genetic distance was calculated as *p*-distance using MEGA 6.06 (Tamura et al., 2013). To determine an appropriate DNA substitution model for maximum likelihood (ML) and Bayesian inference (BI) analyses, we used Akaike information criterion to identify the best-fit model according to jModelTest 2.1.5 (Darriba et al., 2012). The ML analysis was conducted using PhyML version 3.1 (Guindon et al., 2010). BI assessment was performed using MrBayes 3.2.2 (Ronquist et al., 2012).

Variable region 2 on 18S rDNA sequence of *A. milnei* was predicted using ViennaRNA Package (Lorenz et al., 2011). The structure was edited for aesthetic purpose with RnaViz 2.0.3 (De Rijk et al., 2003).

SYSTEMATIC ACCOUNTS

Phylum Ciliophora Doflein, 1901
Class Spirotrichea Bütschli, 1889
Order Stichotrichida Fauré-Fremiet, 1961
Family Amphisiellidae Jankowski, 1979
Genus *Amphisiella* Gourret and Roeser, 1888

***Amphisiella milnei* (Kahl, 1932) Horváth, 1950**
(Table 1, Figs. 1–3)

Holosticha (*Amphisiella*) *milnei* Kahl, 1932: 590.
Amphisiella milnei: Agamaliev, 1972: 22; Aladro-Lubel et al., 1986: 239 and 1990: 127 (cited from Berger, 2008: 118); Berger, 2001: 33; 2008: 118; Li et al., 2016: 59.

Diagnosis. Size *in vivo* about 120×40 μm, elongate rectangular to elliptical; 2 macronuclear nodules; two large and several small ring-shaped structures; yellowish cortical granules 0.8×0.6 μm in size, irregularly arranged on ventral, longitudinally on dorsal side; Usually 37 adoral membranelles; 3 frontal cirri; 1 buccal cirrus; 1 parabuccal cirrus; 2 extra cirri; 3 frontoventral cirri; 35 amphisiellid median cirri; 32 left and 33 right marginal cirri. 5 transverse and 2 pretransverse cirri; 7 dorsal kineties.

Morphological description. *Amphisiella milnei* has a size of 110–130×35–45 μm *in vivo* (120×40 μm on average) and a size of 118×46 μm on average on protargol preparations. They are slightly inflated than living cells due to treatment for impregnation (Table 1). It has flexible body but not contractile (Figs. 1D, 2D). Body shape is elongate rectangular to elliptical, that is, both left and right margins are parallel, with slight convex at left side (Figs. 1A, 2A). Body shows dorsoventrally flatten shape of about 1.7 : 1 ratio (Figs. 1D, 2C).

Nuclear apparatus locates on the left side of mid-body. It consists of two macronuclear nodules with one to five micronuclei. Macronuclear nodules have elliptical shape while micronuclei show spherical shape as in ordinary hypotrichs. Micronuclei usually locate on the up or down side of the macronuclear nodules, not the lateral side of nodules (Figs. 1H, 2I, 3F).

The contractile vacuole was not observed. Cytoplasm is colorless. It contains few yellowish crystals mainly in the posterior body portion. Cyanobacteria and diatoms were observed in food vacuoles. It swims and glides fast at the bottom of Petri dish (Fig. 2K). On ventral side, yellowish cortical granules show dense and irregular arrangement on

Table 1. Morphometric data from *Amphisiella milnei*

Characteristics	Mean	Min	Max	Med	SD	SE	CV	n
Length of body	117.6	88	151	115	14.04	3.62	11.9	15
Width of body	46.0	30	62	46	9.28	2.39	20.2	15
Length of body/width of body	2.6	2	4	3	0.39	0.10	14.8	15
Length of adoral zone of membranelles	44.2	29	52	46	6.28	1.62	14.2	15
Length of adoral zone of membranelles/Length of body (%)	37.9	22.6	44.4	39	5.34	1.38	14.1	15
Length of anteriormost macronuclear nodule	16.0	13	18	16	1.77	0.46	11.0	15
Width of anteriormost macronuclear nodule	9.7	7	11	10	1.09	0.28	11.2	15
No. of macronuclear nodule	2.0	2	2	2	0.00	0.00	0.0	15
Largest diameter of micronucleus	3.0	2	4	3	0.53	0.14	17.8	15
No. of micronuclei	2.1	1	5	2	0.96	0.25	46.5	15
No. of adoral membranelles	36.7	34	40	37	2.02	0.52	5.5	15
Length of largest adoral membranelle	7.9	6	10	8	1.07	0.28	13.5	15
No. of frontal cirri	3.0	3	3	3	0.00	0.00	0.0	15
No. of cirri behind leftmost frontal cirrus	1.9	1	2	2	0.26	0.07	13.4	15
No. of parabuccal cirrus	1.0	1	1	1	0.00	0.00	0.0	15
Distance from anterior body end to buccal cirrus	24.6	20	29	25	2.75	0.71	11.2	15
No. of buccal cirrus	1.0	1	1	1	0.00	0.00	0.0	15
No. of frontoventral cirri	3.0	3	3	3	0.00	0.00	0.0	15
Distance from posterior to rear end of amphisiellid median cirral row	35.2	15	56	35	8.39	2.17	23.9	15
No. of amphisiellid median cirri	27.3	25	31	26	1.88	0.48	6.9	15
No. of left marginal cirri	32.2	27	36	32	2.68	0.69	8.3	15
No. of right marginal cirri	33.1	27	44	33	4.50	1.16	13.6	15
No. of pretransverse cirri	2.0	2	2	2	0.00	0.00	0.0	15
No. of transverse cirri	5.1	5	6	5	0.26	0.07	5.1	15
No. of dorsal kineties	6.7	6	7	7	0.47	0.14	6.9	11

Data based on protargol-impregnated specimens. Measurements in μm.
Mean, arithmetic mean; Min, minimum; Max, maximum; Med, median; SD, standard deviation; SE, standard error of arithmetic mean; CV, coefficient of variation in %; n, number of specimens investigated.

ventral side (Figs. 1E, 2G). On dorsal side, cortical granules form longitudinal groups that composed of several to tens and obliquely arranged as consecutive diagonal lines (Figs. 1F, 2H). Dorsal bristles located between these groups (Figs. 1B, 2H, arrowheads). These granules show as spherical shape (ca. 0.6 μm in diameter) when observed on ventral and dorsal side of the cell (Figs. 1B, 2G, H). However, it was actually elliptical shape (ca. 0.8×0.6 μm) on lateral view (Figs. 1C, 2J). In addition, *Amphisiella milnei* has distinct ring-shaped structures in the cytoplasm (Figs. 1A, 2A, B). These structures are colorless with a size of 3 to 7 μm in diameter. Each individual contains two large and several small ring-shaped structures. The former located at the anterior and posterior regions of body, while the latter are usually scattered in the whole body (Figs. 1A, 2B).

Somatic ciliatures consist of frontal, parabuccal, buccal, frontoventral (anlage IV-origin), marginal, pretransverse, and transverse cirri. These cirri are 8−16 μm long *in vivo*. Most notably, *Amphisiella milnei* has usually two extra cirri located between leftmost frontal cirrus and buccal cirrus (Figs. 1G, 2E, 3C). It is located between rightmost frontal cirrus and frontoventral cirri. Buccal cirrus is located at a level of one third of undulating membranes. The row of frontoventral cirri are located beside the ACR (Figs. 1G shadow marks, 3A, 3C). The amphisiellid median cirri row shows oblique arrangement that commences near the distal end of adoral zone and terminates at two third of the body. The amphisiellid median cirral (Figs. 1G, 3A) and transverse cirri are conspicuously enlarged, showing J-shaped arrangement. The cilia conspicuously protrude the posterior body end (Figs. 1A, 2A, 2F). Two pretransverse cirri are located near the transverse cirri. Usually the right pretransverse cirrus (VI/2) are located more anteriorly than the left one (V/2) (Figs. 1G, 3A, 3E). Right and left marginal cirral rows terminate at the level of pretransverse cirri and the rearmost transverse cirrus, respectively (Figs. 1G, 3A). Marginal rows are distinctly separated posteriorly.

On the dorsal side, there are six to seven bipolar dorsal kineties (Figs. 1H, 3D). Leftmost kinety (dorsal kinety 1) is anteriorly shortened. In protargol-impregnated specimens, dorsal kinety 7 was usually located at the ventral side (Figs. 1G, 3A). Dorsal bristles are 3−4 μm long *in vivo* (Fig. 1B, H).

Oral apparatus occupies usually one third of the body length in protargol-impregnated specimens. Adoral zone is composed of about 37 adoral membranelles. The proximal end of adoral zone is located at the level of middle portion of ACR. Endoral and paroral membranes show parallel arrangement without distinct curve (Fig. 1G).

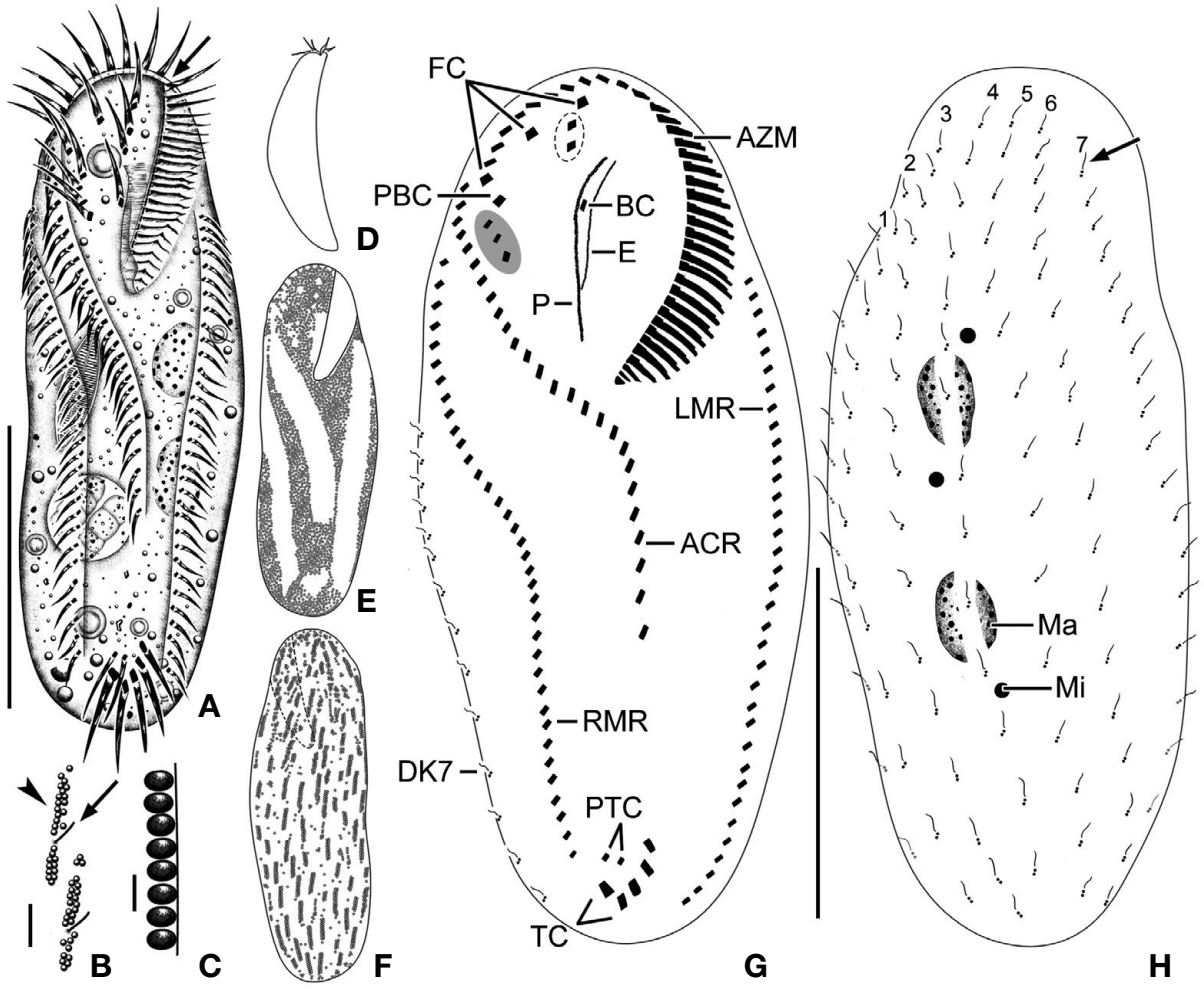

Fig. 1. *Amphisiella milnei* from life (A–F) and after protargol impregnation (G, H). A, Ventral view of a representative specimen and scutum (arrow); B, Dorsal bristles (arrowhead) are arranged between the cortical granules (arrow); C, Cortical granules are elliptical in lateral view; D, Right lateral view of a living specimen; E, F, Cortical granules on ventral and dorsal side; G, H, Ciliature of the ventral and dorsal side; the dash line marks the extra cirri behind leftmost frontal cirrus; the shadow marks the short row of frontoventral cirri; the arrow marks the dorsal bristle. ACR, amphisiellid median cirral row; AZM, adoral zone of membranelles; BC, buccal cirrus; DK, dorsal kineties; E, endoral; FC, frontal cirri; LMR, left marginal row; Ma, macronuclear nodule; Mi, micronucleus; P, paroral; PBC, parabuccal cirrus; PTC, pretransverse cirri; RMR, right marginal row; TC, transverse cirri. Scale bars: A, G = 50 μm, B = 5 μm, C = 1 μm.

Molecular analyses of 18S rDNA sequence. Based on topology obtained from BI and ML analyses, the genus *Amphisiella* can be split into two groups. The first group is composed of *A. annulata* (DQ832260, GU170843), *A. pulchra* (JX 461343), and *A. sinica* (FJ870073) with high supporting values (BI/ML, 1.00/99%). The second group is composed of *A. milnei* (MH645737, FJ870072) and *A. candida* (JX 461344) with high supporting values (BI/ML, 1.00/99%). The family Trachelostylidae branches between the two *amphisiella* groups, which is formed by two genera (Trachelostyla and Spirotrachelostyla) and supported clade with first *amphisiella* group (BI/ML, 0.86/58%) (Fig. 4). Even though Trachelostylidae located between the two groups of *Amphisiella* that could be considered as an intermediate taxon between the two, their supporting values on the tree were slightly low. Considering the position of the family Trachelostylidae on the tree, it does not coincide with Li et al. (2016) and Huang et al. (2016) but the two reports also did not correspond each other.

The variable region 2 on the 18S rDNA sequence is 168 bp in length. Putative secondary structure of this region showed that it was identical to its congener *A. candida*. Only two base changes were observed in single stranded regions (Fig. 5). The structure of *A. milnei* consisted of four helixes:

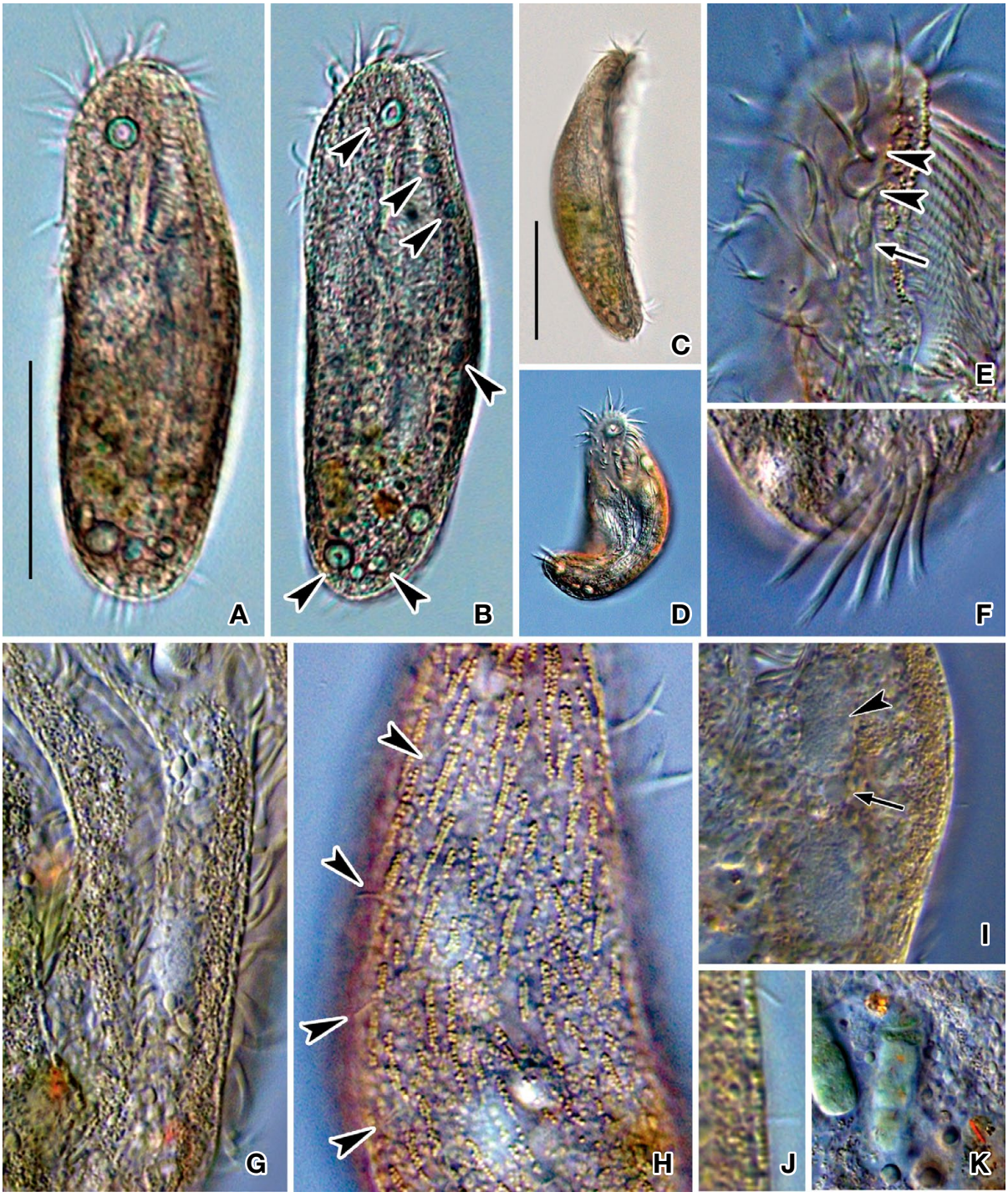

Fig. 2. Photographs of *Amphisiella milnei* from living specimens. A, Ventral view of a typical specimen; B, Various size of ring-shaped structure (arrowheads); C, Right lateral view; D, Specimen showing body flexibility; E, Cirri in anterior body portion; the extra cirri behind leftmost frontal cirrus (arrowheads) and buccal cirrus (arrow); F, Transverse cirri; G, H, Cortical granules on ventral (G) and dorsal side (H); dorsal bristles (arrowheads); I, Macronuclear nodule (arrowhead) and micronucleus (arrow); J, Cortical granules are elliptical in lateral view; K, The cyanobacteria and crystals in food vacuole. Scale bars: A, C = 50 μm.

9, 10, E10-1, and 11. Helix 9 showed one hairpin loop with two internal loops. Helix 10 was composed of one hairpin loop with one internal loop. Helix E10-1 consisted of one hairpin loop with three internal loops. Helix 11 presented

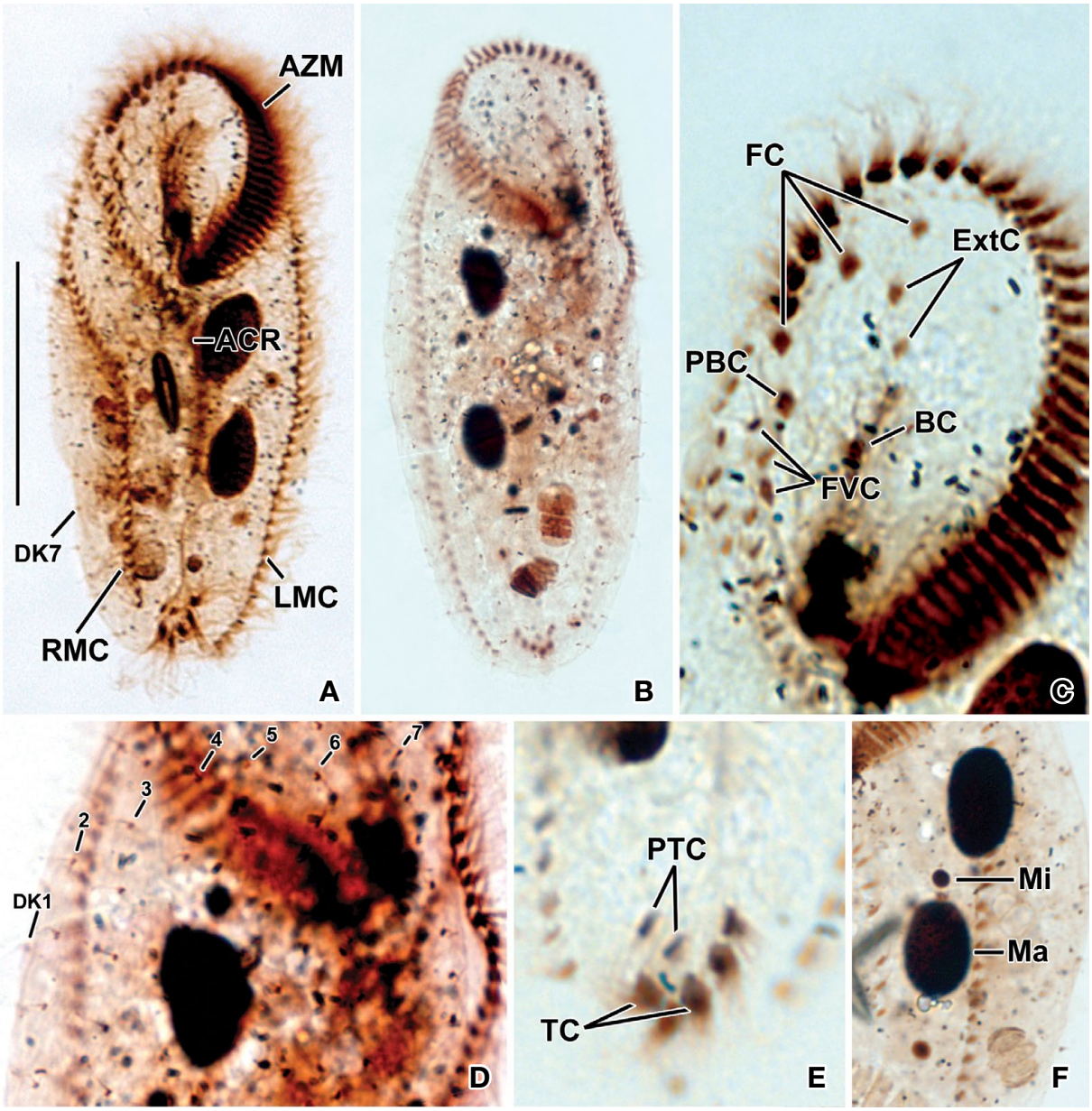

Fig. 3. Photographs of *Amphisiella milnei* after protargol impregnation. A, B, Ventral and dorsal view of representative specimens; C, Anterior body portion of ventral side; D, Dorsal kineties; E, Pretransverse cirri and transverse cirri; F, Nuclear apparatus. ACR, amphisiellid median cirral row; AZM, adoral zone of membranelles; BC, buccal cirrus; DK, dorsal kineties; ExtC, extra cirri behind leftmost frontal cirrus; FC, frontal cirri; FVC, frontoventral cirri; LMC, left marginal row; Ma, macronuclear nodule; Mi, micronucleus; PBC, parabuccal cirrus; PTC, pretransverse cirri; RMC, right marginal row; TC, transverse cirri. Scale bar: A=50 μm.

one hairpin loop with one bulge. Of six internal loops, two were asymmetric while the others were symmetric.

Distribution. Apseronskij and Bakinskij archipelagos (Caspian Sea), China, Germany, Mexico, and Korea (present study).

Remarks. The genus *Amphisiella* consists of the following eight species: *Amphisiella capitata* (type species), *A. annulata*, *A. candida*, *A. milnei*, *A. ovalis*, *A. pulchra*, *A. sinica*, and *A. turanica*. Only A. milnei has extra cirri among members in the genus *Amphisiella* for which populations have been described based on live observation and protargol-impregnated specimen (Kahl, 1932; Agamaliev, 1972; Li et al., 2016). However, the illustration of *A. capitata* provided by Pereyaslawzewa (1886) appeared to have extra cirri at

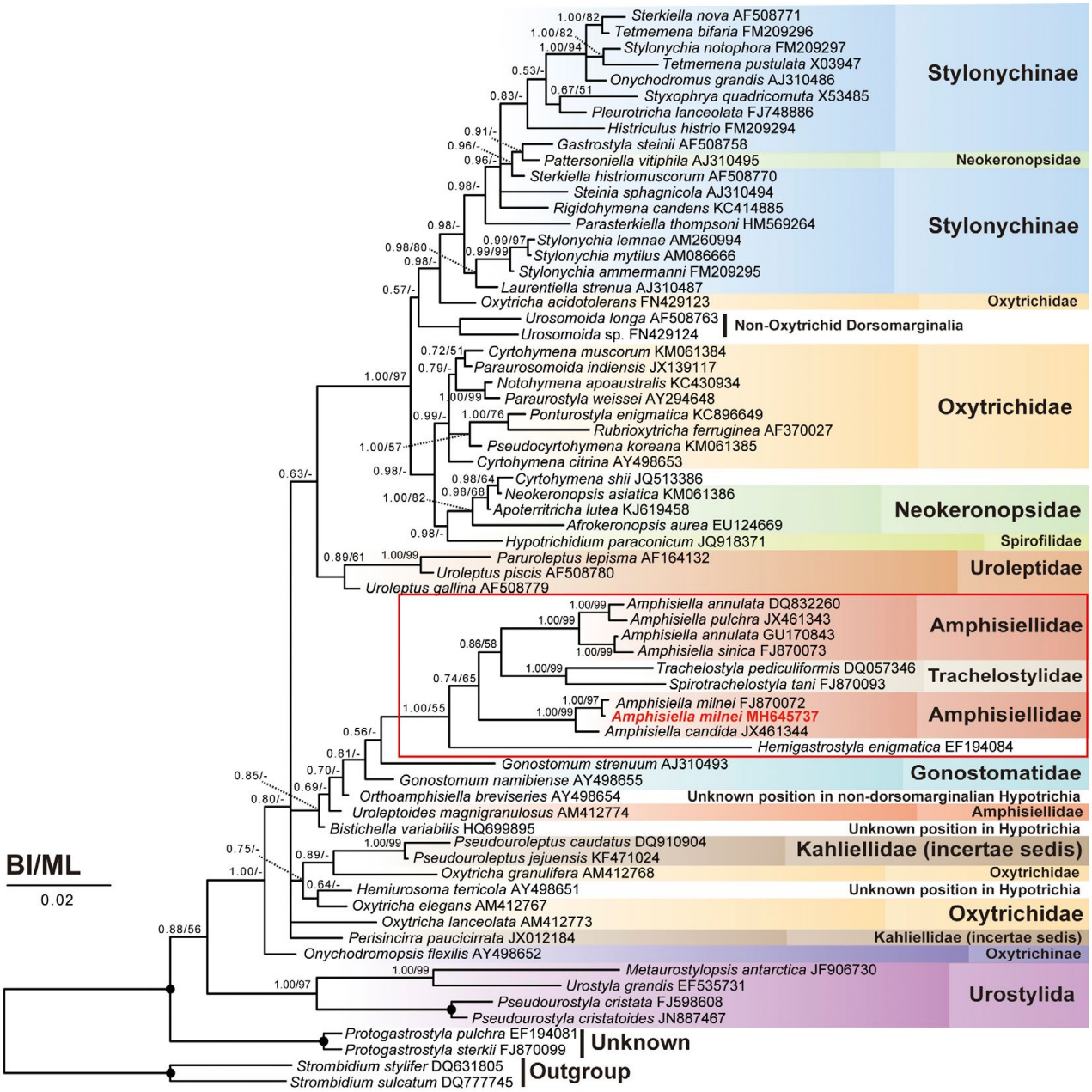

Fig. 4. Maximum likelihood (ML) and Bayesian (BI) phylogenetic tree based on small subunit (SSU) rRNA gene sequences of 68 hypotrichous ciliates. Node labels indicate the BI posterior probabilities followed by ML bootstrap values; a dash denotes a value of below 0.50 (BI) or 50% (ML); a solid circle denotes a fully supported (1.00/100%) branches. The scale bar corresponds to three substitutions per 100 nucleotide positions. The new species is denoted as red in color and bold.

the same position based on live observation which might be over-interpreted. Recently, *A. marioni* sensu Li et al., 2007 was re-described using silver impregnation. It was synonymised as *A. capitata* as this population lacked extra cirri (Li et al., 2007).

For *Amphisiella milnei* (Kahl, 1932) Horváth, 1950, here we compare three populations separately (Table 2). Based on the original description (Kahl, 1932), this species has extra cirri behind the leftmost frontal cirrus with two or three extra cirri. The type population differs from the Korean population (this study) by ring-shaped structure (two rings each in anterior and posterior body potion vs. two rings each in anterior and posterior portion with additional rings in marginal portion), cortical granules (one colorless and one yel-

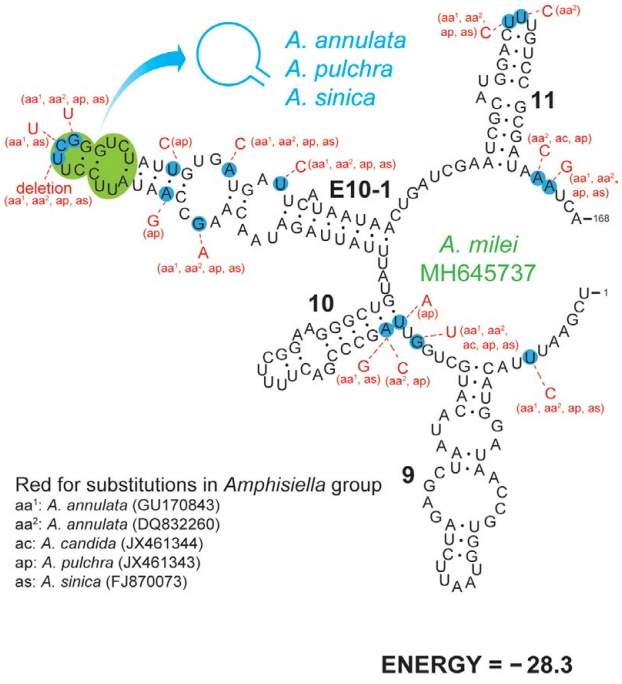

Fig. 5. Secondary structure of 18S rDNA sequence (variable region 2) of *Amphisiella milnei*. Substitutions on *A. candida* (red) and structural difference with *A. annulata*, *A. pulchra*, and *A. sinica* (green) are denoted as blue color.

lowish granules vs. single type of yellowish granules), parabuccal (absent based on illustration vs. present), frontoventral (two based on illustration vs. three), ACR (terminated at near transverse cirri vs. at 2/3 fo body length), marginal cirral rows (terminated at posterior body end vs. at the level of pretransverse and transverse cirri), and pretransverse cirri (absent based on illustration vs. present). *Amphisiella minei* sensu Agamaliev, 1972 differs from Korean population by ACR (terminated at near transverse cirri vs. at 2/3 of body length), marginal cirral rows (terminated at posterior body end vs. at the level of pretransverse and transverse cirri), amphisiellid median and left marginal cirri (about 38 and 44 based on illustration vs. 25−31 and 27−36), and pretransverse cirri (absent based on illustration vs. two). Agamaliev's specimen might have been stained with inappropriate impregnation method (Berger, 2008). Thus, the frontal region is not comparable to the Korean population. Of these three populations, only the Chinese population can be compared in detail. There are minor differences between the Chinese and Korean populations (Li et al., 2016): (1) ring-shaped stucture (usually two large vs. two large and several small); (2) anteriormost pretransverse cirrus (almost horizotal level vs. VI/2); and (3) three nucleotdie differenence of 18S rDNA and 99.9% genetic distance (*p*-distance). This supports that they are conspecific.

Table 2. Morphological comparison of *Amphisiella milnei*

Character	German population	Caspian Sea population	Chinese population	Korean population
Body, length (μm)	100–140[a]	ca. 120[b]	92–144	88–151
Ring-shaped structures, number	Usually two large	–	Usually two large	Usually two large and several small
Cortical granules type	Two types	–	Single type	Single type
Cortical granules color and size (μm)	Colourless and yellowish (size was not mentioned)	–	Light yellowish (ca. 0.5)	Yellowish (ca. 0.6)
BC, level	Beside PM	Beside PM	Beside PM	Beside PM
BC, number	8–10[c]	6–9[c]	1	1
FC, number	–	–	3	3
PBC, number	–	–	1	1
Cirri behind leftmost FC, number	–	–	1–3	1–2
Frontoventral cirri, number	–	–	3	3
PTC, number	Absent[d]	Absent[d]	2	2
Anteriormost PTC	–	–	Almost horizontal	VI/2
Reference	Kahl (1932)	Agamaliev (1972)	Li et al. (2016)	Present study

All most measured data are based on protargol-impregnated specimens.
–, not described; BC, buccal cirrus; PM, paroral membrane; FC, frontal cirri; PBC, parabuccal cirrus; PTC, pretransverse cirri.
[a]Data from living specimen.
[b]It was not mentioned whether life or protargol-impregnation.
[c]Cirri on anterior body portion was not clearly separated on the description. Thus, the number of cirri included all cirri on that area without separation.
[d]Data based on illustrations.

ACKNOWLEDGMENTS

This research was supported by KIOST projects (PE99624).

REFERENCES

Agamaliev FG, 1972. Ciliates from microbenthos of the islands of Apšeronskij and Bakinskij archipelagos of the Caspian Sea. Acta Protozoologica, 10:1-27.

Berger H, 2001. Catalogue of ciliate names 1. Hypotrichs. Verlag Helmut Berger, Salzburg, pp. 1-206.

Berger H, 2008. Monograph of the Amphisiellidae and Trachelostylidae (Ciliophora, Hypotricha). Monographiae Biologicae, 88:1-737. https://doi.org/10.1007/978-1-4020-8917-6

Chen X, Shao C, Lin X, Clamp JC, Song W, 2013. Morphology and molecular phylogeny of two new brackish-water species of *Amphisiella* (Ciliophora, Hypotrichia), with notes on morphogenesis. European Journal of Protistology, 49:453-466. https://doi.org/10.1016/j.ejop.2012.11.002

Darriba D, Taboada GL, Doallo R, Posada D, 2012. jModelTest 2: more models, new heuristics and parallel computing. Nature Methods, 9:772. https://doi.org/10.1038/nmeth.2109

De Rijk P, Wuyts J, De Wachter R, 2003. RnaViz 2: an improved representation of RNA secondary structure. Bioinformatics, 19:299-300. https://doi.org/10.1093/bioinformatics/19.2.299

Drummond A, Ashton B, Buxton S, Cheung M, Cooper A, Duran C, Field M, Heled J, Kearse M, Markowitz S, Moir R, Stones-Havas S, Sturrock S, Thierer T, Wilson A, 2014. Geneious v7.1.5. created by Biomatters. Biomatters, Auckland.

Foissner W, 1991. Basic light and scanning electron microscopic methods for taxonomic studies of ciliated protozoa. European Journal of Protistology, 27:313-330. https://doi.org/10.1016/S0932-4739(11)80248-8

Guindon S, Dufayard JF, Lefort V, Anisimova M, Hordijk W, Gascuel O, 2010. New algorithms and methods to estimate maximum-likelihood phylogenies: assessing the performance of PhyML 3.0. Systematic Biology, 59:307-321. https://doi.org/10.1093/sysbio/syq010

Huang J, Luo X, Bourland WA, Gao F, Gao S, 2016. Multigene-based phylogeny of the ciliate families Amphisiellidae and Trachelostylidae (Protozoa: Ciliophora: Hypotrichia). Molecular Phylogenetics and Evolution, 101:101-110. https://doi.org/10.1016/j.ympev.2016.05.007

Jung JH, Min GS, 2009. New record of two species in stichotrichous ciliates (Ciliophora: Stichotrichia) from Korea. Korean Journal of Systematic Zoology, 25:227-236. https://doi.org/10.5635/KJSZ.2009.25.3.227

Jung JH, Park KM, Min GS, 2012. Morphology, morphogenesis, and molecular phylogeny of a new brackish water ciliate, *Pseudourostyla cristatoides* n. sp., from Songjiho lagoon on the coast of East Sea, South Korea. Zootaxa, 3334:42-54.

Kahl A, 1932. Urtiere oder Protozoa I: Wimpertiere oder Ciliata (Infusoria). 3. Spirotricha. Tierwelt Deutschlands, 25:399-650.

Li J, Lin X, Shao C, Gong J, Hu X, Song W, 2007. Morphological redescription and neotypification of the marine ciliate, *Amphisiella marioni* Gourret & Roeser, 1888 (Ciliophora: Hypotrichida), a poorly known form misidentified for a long time. Journal of Eukaryotic Microbiology, 54:364-370. https://doi.org/10.1111/j.1550-7408.2007.00270.x

Li L, Zhao X, Ji D, Hu X, Al-Rasheid KAS, Al-Garraj SA, Song W, 2016. Description of two marine amphisiellid ciliates, *Amphisiella milnei* (Kahl, 1932) Horváth, 1950 and *A. sinica* sp. nov. (Ciliophora: Hypotrichia), with notes on their ontogenesis and SSU rDNA-based phylogeny. European Journal of Protistology, 54:59-73. https://doi.org/10.1016/j.ejop.2016.04.004

Lorenz R, Bernhart SH, zu Siederdissen CH, Tafer H, Flamm C, Stadler PF, Hofacker IL, 2011. ViennaRNA Package 2.0. Algorithms for Molecular Biology, 6:26. https://doi.org/10.1186/1748-7188-6-26

Lynn DH, 2008. The ciliated protozoa: characterization, classification, and guide to the literature. 3rd ed. Springer, New York, pp. 1-605.

Notredame C, Higgins DG, Heringa J, 2000. T-coffee: a novel method for fast and accurate multiple sequence alignment. Journal of Molecular Biology, 302:205-217. https://doi.org/10.1006/jmbi.2000.4042

Pereyaslawzewa S, 1886. Protozoaires de la mer Noire. Zapiski Novorossiiskago Obshchestva Estestvoispytatelei, 10:79-114.

Ronquist F, Teslenko M, van der Mark P, Ayres DL, Darling A, Höhna S, Larget B, Liu L, Suchard MA, Huelsenbeck JP, 2012. MrBayes 3.2: efficient Bayesian phylogenetic inference and model choice across a large model space. Systematic Biology, 61:539-542. https://doi.org/10.1093/sysbio/sys029

Sonnenberg R, Nolte AW, Tautz D, 2007. An evaluation of LSU rDNA D1-D2 sequences for their use in species identification. Frontiers in Zoology, 4:6. https://doi.org/10.1186/1742-9994-4-6

Tamura K, Stecher G, Peterson D, Filipski A, Kumar S, 2013. MEGA6: molecular evolutionary genetics analysis version 6.0. Molecular Biology and Evolution, 30:2725-2729. https://doi.org/10.1093/molbev/mst197

Wilbert N, 1975. Eine verbesserte Technik der Protargolimprägnation für Ciliaten. Mikrokosmos, 64:171-179.

Received November 22, 2017
Revised July 19, 2018
Accepted July 20, 2018